

Orientation-dependent mechanical responses in Mo-Re alloys evaluated via micro-pillars

Hailong Xu¹, Li huang¹, Wen Zhang¹, Jing Liang¹, Xuan Gao¹, and Jianfeng Li¹

¹Northwest Institute for Non-ferrous Metal Research

September 14, 2023

Abstract

Textures in Molybdenum-Rhenium alloys are inevitable during thermal fabrication. [110] and [100] are common orientations in Molybdenum-Rhenium alloys and effect mechanical responses. However, orientation dependence of mechanical responses in Molybdenum-Rhenium alloys is not quite clear yet. To clarify this problem, micro-pillar compression tests are conducted in grains with orientation [100] and [110] separately. Orientation-dependent compressive properties are found in Mo-14Re and Mo-42Re, but are not found in Mo and Mo-5Re, which may be attributed to activated multi-slip planes as increased Re. Solid solution effect of Re not only rely on orientations, but also on Re content. Softening effect occurs in both [100] and [110] Mo-5Re. while, strong strengthening effect happens in [110] Mo-14Re and Mo-42Re. Our research clarifies that Mo-Re alloys with [110] orientation / texture could be preferred to obtain good strengthening effect.

Orientation-dependent mechanical responses in Mo-Re alloys evaluated via micro-pillars

Hailong Xu^{a,b*}, Li Huang^b, Wen Zhang^b, Jing Liang^b, Xuanqiao Gao^b, Jianfeng Li^b

^aXi'an Jiao Tong University, HARCC, State Key Lab Mech Behav Mat, Xi'an 710049, Shaanxi, Peoples R China.

^bNorthwest Institute for Nonferrous Metal Research, Xi'an 710016, China.

*Corresponding author: xuhlnin@163.com

Abstract

Textures in Molybdenum-Rhenium alloys are inevitable during thermal fabrication. [110] and [100] are common orientations in Molybdenum-Rhenium alloys and effect mechanical responses. However, orientation dependence of mechanical responses in Molybdenum-Rhenium alloys is not quite clear yet. To clarify this problem, micro-pillar compression tests are conducted in grains with orientation [100] and [110] separately. Orientation-dependent compressive properties are found in Mo-14Re and Mo-42Re, but are not found in Mo and Mo-5Re, which may be attributed to activated multi-slip planes as increased Re. Solid solution effect of Re not only rely on orientations, but also on Re content. Softening effect occurs in both [100] and [110] Mo-5Re. while, strong strengthening effect happens in [110] Mo-14Re and Mo-42Re. Our research clarifies that Mo-Re alloys with [110] orientation / texture could be preferred to obtain good strengthening effect.

Keywords

Molybdenum-Rhenium alloys; Pillar compression; Mechanical properties; Orientation-dependent

Introduction

Molybdenum (Mo) and molybdenum alloys have stable body-centered cubic (BCC) structure at a large temperature range, which makes Mo alloys wide application in high temperature environment ^[1,2]. However,

high ductile to brittle transition temperature (DBTT) leads poor ductility and processing ability at room temperature in most Mo alloys [3]. One of effective methods to improve processing ability is adding Re to Mo alloys^[4,5]. Leichtfried et al justified the Charpy ductile-to-brittle transition temperature decreased monotonically with increasing rhenium concentration [6]. Combining the cost and strengthening effect of Re element, Re contents in commercial molybdenum alloys are often set as 5wt.%, 14 wt.% and 42 wt.%, respectively [6].

In most cases, thermal mechanical processes are necessary in Mo alloys processes [7,8], including thermal rolling, forging, et al. On one hand, thermal mechanical processes could effectively enhance ductility and facilitate proceeding ability^[9]. On the other hand, textures with specific orientations occur during thermal mechanical processes^[10].

Textures have large effects on the mechanical properties of Mo alloys^[9,10]. According to Xing's results, two grain orientations of $\langle 111 \rangle$ fiber & $\langle 100 \rangle$ fiber and $\langle 100 \rangle$ fiber & $\langle 110 \rangle$ fiber are formed in the 47% and 95% rolled molybdenum sheets, respectively [10]. In Lobanov's results, the molybdenum texture consisted of a set of stable $\langle 110 \rangle$ orientations^[11]. Brittle characteristics show typical cleavage failure in Mo alloys with specific textures. However, It is hard to evaluate individually how textures effect the mechanical properties of Mo-Re alloys via traditional test methods. Here, we propose to clarify this problem via micro-pillar tests.

A lot of researches have been made to investigate orientation-dependent mechanical properties of Mo [12-16]. Schneider et al have verified that small-scale Mo pillars exhibit a strain rate sensitivity similar to bulk Mo, suggesting Mo pillars could evaluate mechanical properties of bulk Mo well [12]. Kim et al have studied that molybdenum nano-pillars exhibit tension-compression asymmetry on [001] and [011] oriented samples [14,15]. Size-dependent mechanical responses in Mo are likely due to the relative shortage of screw dislocations [13]. Mechanical properties in micro-pillars are similar to bulk Mo as the diameter of pillars larger than $2\mu\text{m}$ [16]. In this research, micro-pillars with orientation [100] and [110] are prepared via FIB methods, respectively, to investigate the effects of textures on mechanical responses of Mo-Re alloys.

Experiments

High purity molybdenum powders and rhenium powders were used to prepare Mo-Re alloys. These powders processed via mixing, pressing and sintering to form as sintered Mo-Re alloys. The contents of Re were designed as 5wt.%, 14wt.%, and 42wt.%. These Mo-Re alloys are abbreviated as Mo-5Re, Mo-14Re, and Mo-42Re, respectively. Thermal extrusion with ratio 4:1 was given to reduce geometrical size. Then, thermal annealing at 1100 was conducted to eliminate processed stress.

The as-annealed samples were firstly mechanically grinded and polished to obtain grain sizes under optical microscope. Secondly, Electron Backscatter Diffraction (EBSD JSM-7200F) was used to characterize the grains with [100] and [110] orientations in all samples. Then, pillars with diameter $2\mu\text{m}$ and height-diameter ratio 2:1 were compared via focused-ion-beam (FIB). Finally, compression tests were conducted at room temperature under nano-indentation with a flat indenter. The diameter of indenter is $20\mu\text{m}$ that is much larger than the diameter of sample. The strain rate and final strain were set as $1.67 \times 10^{-3} \text{s}^{-1}$ and 25%, respectively for all tests. At least two samples were tested in same experimental condition to ensure the results.

The surfaces of compressive samples were characterized via scanning electron microscope (SEM). Microstructural details after deformation were characterized by transmission electron microscopy (TEM, JEOL JEM-2100F) at 200KV. The samples for TEM tests were prepared via FIB methods. The distribution of composed elements is detected by energy dispersive spectrometer (EDS) operating at TEM.

Experimental results

Figure 1 shows the metallographs for as-annealed Mo, Mo-5Re, Mo-14Re, and Mo-42Re. Recrystallization occurs in Mo and Mo-5Re because small and round grains forming in the grain boundaries, as shown in Figure 1a and 1b. It is noted that the grain sizes in Mo and Mo-5Re are similar. Thus, the addition of 5wt.% Re has little effect on grain growth. The processed stresses in Mo-14Re and Mo-42Re have not been

totally released, which may be contributed to the enhanced recrystallization temperature. The grain size in Mo-42Re is smaller than in Mo-14Re. In short, grain sizes in all samples are several tens micrometers that is suitable to pillar preparation.

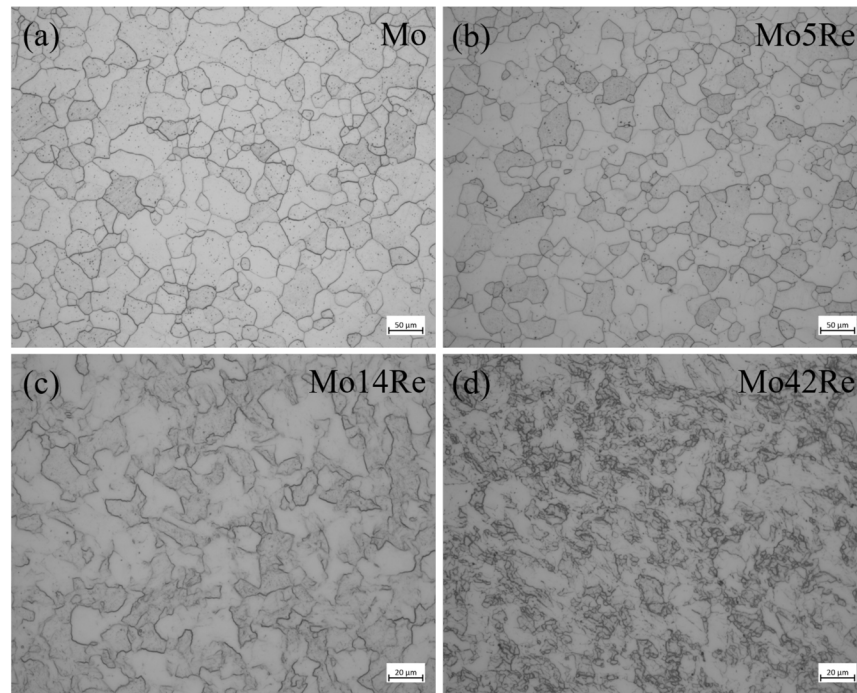


Figure 1 Metallographs for as annealed Mo in (a), Mo-5Re in (b), Mo-14Re in (c) and Mo-42Re in (d).

As shown in Figure 2a and 2b, the orientation in red grains is [100], in green grains is [110]. Grain with 111 orientation is rarely observed in Mo-14Re and Mo-42Re, meaning textures form during thermal extrusion. The grain size in Mo-42Re is much smaller than in Mo-14Re, suggesting evident grain-finishing effect of Re in Mo alloys. Irregular grain boundaries verify that no obvious crystallization occurs. The inserts in Figure 2 show the micrographs of pillar with diameter 2 μm and height 4 μm.

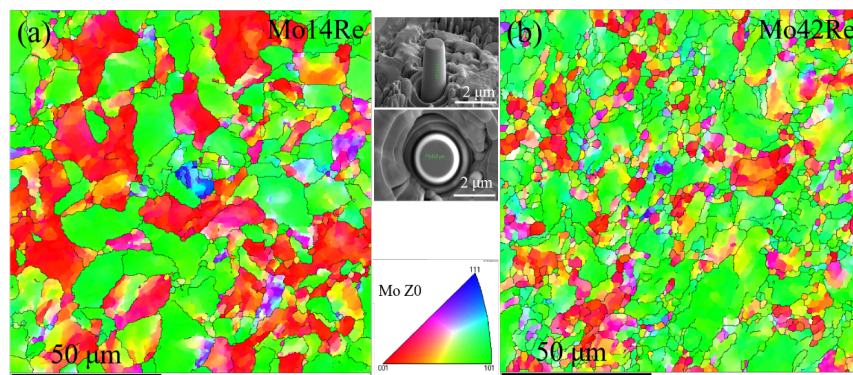


Figure 2 EBSD results for Mo-14Re in (a) and Mo-42Re in (b).

Representative true stress-true strain curves of Mo, Mo-5Re, Mo-14Re and Mo-42Re are shown in Figure 3. Grains with [100] and [110] orientations are tested for each sample. In Figure 3a, Mo grains with [100]

and [110] orientations show different mechanical responses. The yield stresses (~ 400 MPa) are similar in [100] Mo and [110] Mo. However, mechanical responses after yield are different. Strong stress drops appear as strain reach to 2.5% in [110] Mo, suggesting strong local stress release. Strain step for the stress drop is $\sim 1\%$ within 17.5% strain, and increases gradually as strain higher than 17.5%. Following the stress drops to zero, stress rises immediately and reaches a new stress peak in [110] Mo, as shown in Figure 3a. The stress in [100] Mo is much more stable than in [110] Mo, as shown in the red curve in Figure 3a. The flow stress in [100] Mo maintains at a stable level ~ 500 MPa. The different response suggests grain with [100] orientation possesses more stably deformation ability than with [110] Mo.

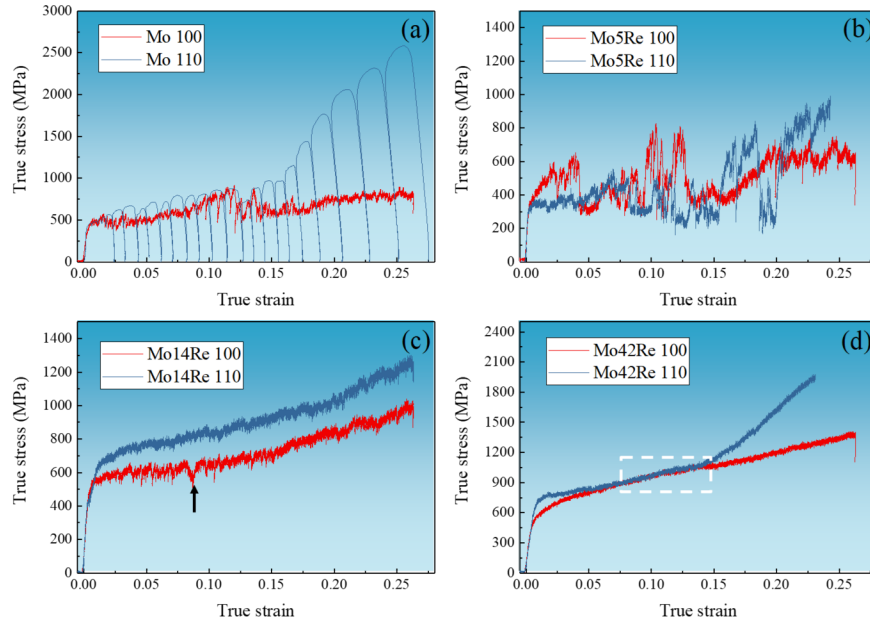


Figure 3 Representative true stress-true strain curves for both [100] and [110] Mo in (a), Mo-5Re in (b), Mo-14Re in (c) and Mo-42Re in (d).

True stress-true strain curves of [110] and [100] Mo-5Re coincide in elastic region, as shown in Figure 3(b). [110] Mo-5Re and [100] Mo-5Re both yield at true stress ~ 300 MPa that lower than Mo, suggesting softening effect happens in Mo-5Re. After yield, true stress in [100] Mo-5Re gradually rises from 300MPa to ~ 600 MPa as true strain reaches 2.5%. Then, stress drops from ~ 600 MPa to ~ 300 MPa at strain 5%. Whereas, [110] Mo-5Re maintains flow stress at ~ 400 MPa from yield point to 7.5% strain. As strain higher than 10%, stress fluctuations emerge strongly in both [100] and [110] Mo-5Re.

Figure 3c shows mechanical responses of [100] and [110] Mo-14Re. The yield stress in [110] Mo-14Re is higher than in [100] Mo-14Re, which is differ with Mo and Mo-5Re. The true stress in [110] Mo-14Re is always higher than in [100] Mo-14Re from yield point to 25%. It is noted that stress drop behaviors are much less distinct in Mo-14Re than in Mo and Mo-5Re, showing the plastic deformation in Mo-14Re is more stable than in Mo-5Re and Mo. What is more, true stress gradually increases from strain 2.5% to 25% in both [110] and [100] Mo-14Re, expect for a slight stress drop from 600MPa to 500MPa. The final stress reaches 1200MPa in [110] Mo-14Re, and 800MPa in [100] Mo-14Re at strain $\sim 25\%$.

The true stress-true strain curves of [100] and [110] Mo-42Re are shown in Figure 3d. The stress in [110] Mo-42Re is higher than in [100] Mo-42Re at yield point. The stress in [110] Mo-42Re maintains at steady level from 1% to 5%. While in this region, the stress in [100] Mo-42Re rises from 450MPa to 750MPa. Two curves overlap within 7.5% to 15%, as shown in the white dotted square in Figure 3d. As strain continually increases, the stress in [110] Mo-42Re rapidly enhances to 2000MPa from 15% to 25%. The stress in [100]

Mo-42Re, however, steadily rises to 1200MPa. The stress drops behaviors in Mo-42Re is much smoother than in Mo-14Re.

Figure 4a shows the results for Mo, Mo-14Re and Mo-42Re with [100] orientation. Yield strength enhances with Re content rises. Besides, the stress at 25% strain is effectively improved in [100] Mo-42Re, which means strong hardening effect. An outstanding feature is that stress drop behaviors weaken as Re content increases, both in samples with [100] orientation (Figure 4a) and with [110] orientation (Figure 4b). The stresses are adjacent in [110] Mo-14Re and Mo-42Re in the stain region between 2% to 10%. As strain higher than 15% in [110] samples, stresses in Mo and Mo-42Re begin to rapidly increases. Such a behavior may be induced via large changing shape of samples.

Figure 4 The true stress-true strain curves of Mo, Mo-14Re and Mo-42Re with [100] orientation in (a) and with [110] orientation in (b). (c) is the summary of yield stresses.

Figure 5 shows the surface micrographs of samples after compression with true strain 25%. Only one group of parallel slip bands emerge in [100] Mo and Mo-14Re, as shown in Figure 5a and 5c. [110] Mo still behaviors strong slips along a single slip plane. Two groups of slips bands tangles in [100] Mo-42Re, which may lead to strengthening effect. Plastic deformation in [110] Mo-14Re and Mo-42Re are dominated by multi-slip bands. Asymmetric deformation leads inclination in [100] Mo-42Re, as seen in Figure 5e.

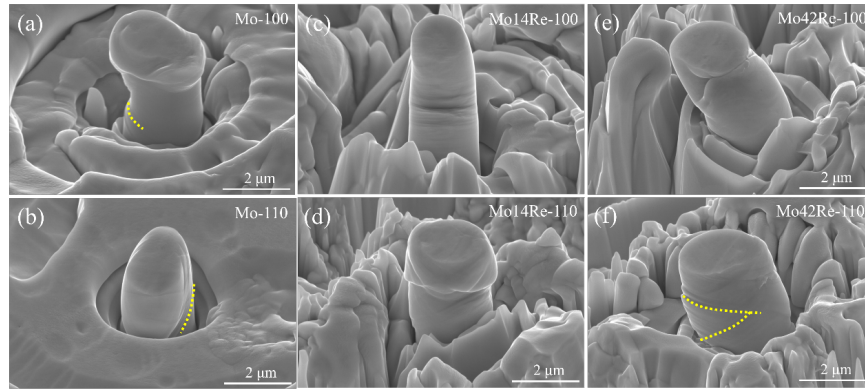


Figure 5 Surface micrographs of pillars after compression with true strain 25%. (a), (c) and (e) are [100] Mo, [100] Mo-14Re and [100] Mo-42Re, respectively. (b), (d) and (f) are [110] Mo, [110] Mo-14Re, and [110] Mo-42Re, respectively.

To analyze the effect of Re content on compression behavior, [100] Mo and Mo-42Re are observed via TEM, as shown in Figure 6. TEM samples are prepared via FIB methods to get a thin cross-sectional region. The view directions are signed in Figure 6a and 6e. One group of parallel slip bands within high density dislocations are observed in [100] Mo, as marked in Figure 6b. The beam direction is [110], as shown in Figure 6c. Figure 6d is the magnification of region B in Figure 6b, in which dislocations are nearly free at the bottom region. Thus, plastic deformation takes place locally in slip bands and rarely in other parts of the [100] Mo pillar.

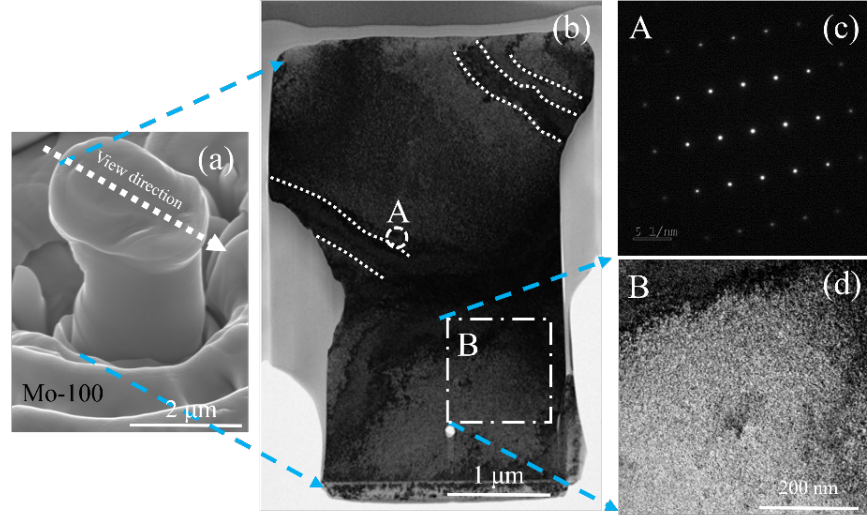


Figure 6 Cross-sectional TEM results of compressive [100] Mo in (a), (b), (c) and (d).

To compare the orientation on the mechanical responses, TEM results for deformed [100] and [110] Mo-14Re are presented in Figure 7 with beam direction [110]. Only one group of parallel slips are signed in Figure 7b. The region including slips is enlarged in Figure 7d. Although Figure 7d shows contrast, no obvious element segregation occurs in the boundary. Severe shear instability is observed in [110] Mo-14Re in Figure 7f. Shear offset in the free surface cumulates to width $\sim 1\mu\text{m}$ via one group of bands slipping. Although another group of slip bands extend from left side, as shown in region C in Figure 7f, two groups slip bands extend individually. So, the deformations in [100] and [110] Mo-14Re are both mainly dominated by slipping in one group of parallel bands, although slip bands with other directions are activated in [110] Mo-14Re. As above-mentioned, the plastic deformation in [100] Mo-42Re is dominated by tangled slip bands, which suggests plasticity is enhanced as Re rises.

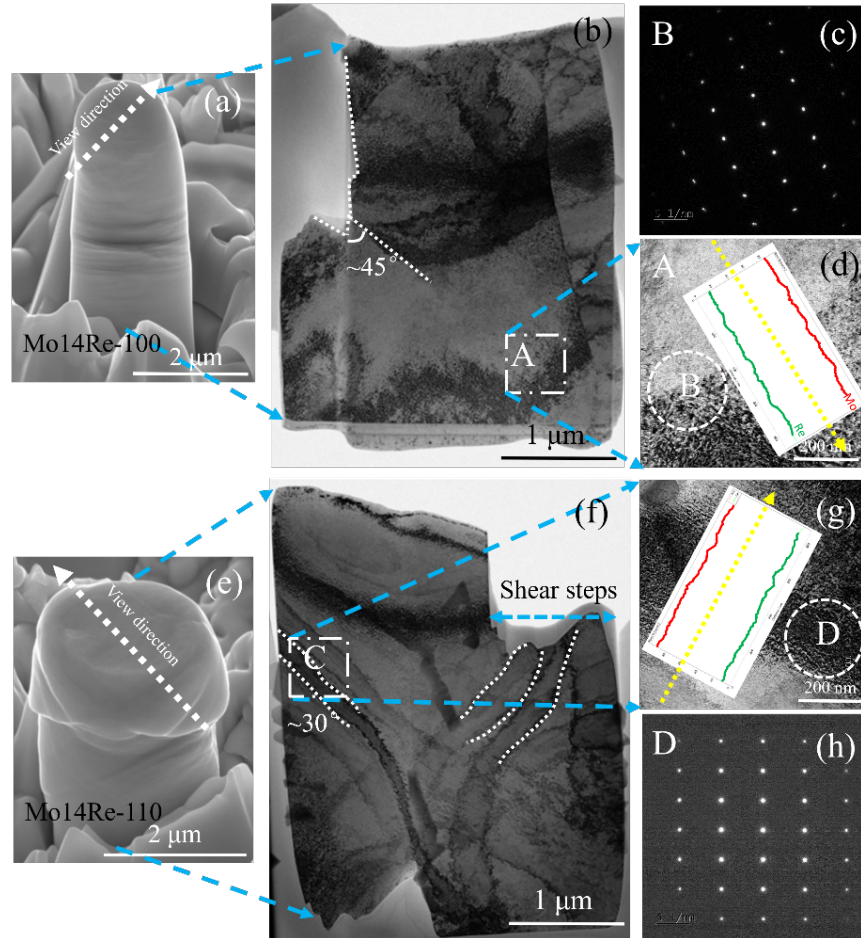


Figure 7 Cross-sectional TEM results of compressive [100] Mo-14Re in (a), (b), (c) and (d). The results of [110] Mo-14Re in (e), (f), (g) and (h).

Distinguishing with un-uniform deformation in [110] Mo-14Re, the drum type of deformed [110] Mo-42Re pillar is shown in Figure 8a and 8b. Two groups of slip bands tangle and leave steps behind, as illustrated in the dotted rectangle in Figure 8a. Several curved slip bands are observed in Figure 8b. Region C is magnified in Figure 8c where one slip band divides into two slips and cross low-angle grain boundary. The disorientation between region D and E is $\sim 10^\circ$, as shown in Figure 8d. Slip bands are hindered when extend to the grain boundary, which induces another slip band is activated to release stress concentration. Thus, adding Re to Mo strikingly enhances dislocation nucleation in grains with [110] orientation.

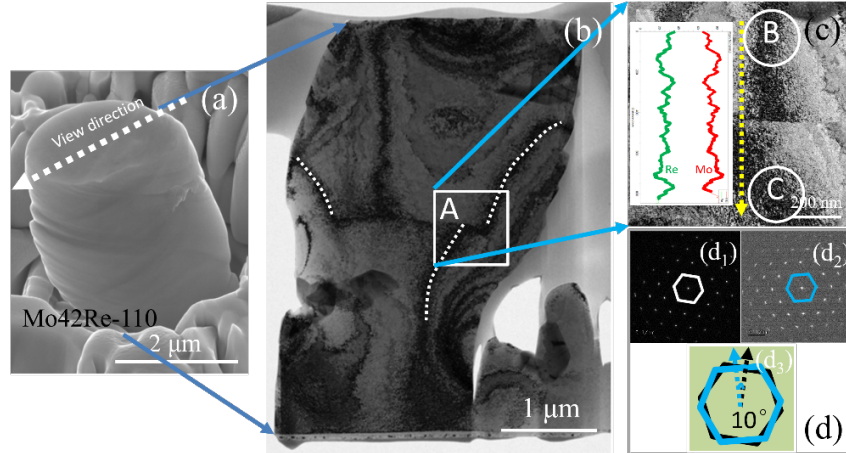


Figure 8 Cross-sectional TEM results of compressive [110] Mo in (a), (b), (c) and (d).

Discussion

The mechanical responses of Mo-Re pillars not only depend on the orientation of grain, but also on Re content, as displayed in Figure 9. Mo and Mo-5Re show weak orientation-dependent behavior. Yield stresses in [100] Mo and Mo-5Re are near to the corresponding [110] ones. In Mo-14Re and Mo-42Re, however, [110] samples are much stronger than [100] samples. The addition of 5wt.% Re soften Mo and lead lower yield stresses in Mo-5Re than in Mo. While, 14wt.% and 42wt.% Re could effectively enhance deformation resistance. [100] Mo shows similar yield stress with [110] Mo, which is inconsistent with previous researches in Mo. Lots of micro-pillar tests in BCC metals have been in Kim's researches and been widely cited^[14,15,17]. In their results, compressive yield stresses in [100] Mo are much higher than in [110] Mo^[15]. The divergence may be due to the size difference that diameters in this work are much larger than other researches.

Figure 9 Summary of yield stresses for [100] and [110] Mo and Mo-Re alloys.

Slip planes in pure Mo that is easily activated at room temperature are {110}^[18,19]. For example, Kim et al. examined the slip traces in niobium pillars using SEM and found the planes to generally agree with {110} slip for their (001) oriented pillars in both tension and compression^[17]. As illustrated in Figure 6 and figure 7, the normal direction of slip planes in [100] Mo and Mo-14Re are both nearly 45°, meaning activated slip places likely to be {110}. The slip planes in [110] Mo-14Re and Mo-42Re may also be {110}, as shown in Figure 7e and Figure 8. Thus, {110} slip systems dominate plasticity in both [100] and [110] Mo and Mo-Re alloys. One group of parallel slip planes activated in [100] and [110] Mo, which may be attributed to the severe shear instability in [110] Mo. Surface micrographs of pillars after compression in [100] Mo-14Re and Mo-42Re exhibit similar slip features, as shown in Figure 5. Two groups of slip planes activated in [110] Mo-14Re, but do not tangle together, as shown in Figure 7f. Multi-slip bands activate and tangle in deformed [110] Mo-42Re, which effectively improve compressive properties. Therefore, the activation of multi-slip systems becomes easier as Re content rises.

Medvedeva et al. have theoretically justified that Re lead solid solution softening in Mo, because non-planar core of the screw dislocation in Mo tends to a planar core under alloying with Re^[20]. In experimental results, however, solid solution effect of 5wt.% Re on Mo depends on processed states. Distinct solid solution softening effect happens in both as-worked and stress-relieved Mo-5Re, but does not happen in fully recrystallized ones^[6]. In this research, full recrystallization occurs in Mo-5Re after 1100 annealing, as shown in Figure 1. It is noted that no microstructural defects such as grain boundary segregation in micro-pillars. Thus, less defects in Mo-5Re pillars may induce mechanical response near to theoretical simulation. Solid solution effect changes as increased Re^[20,21]. As shown in Figure 9, hardening effects in [100] Mo-14Re and Mo-42Re are

quite weak, which is consistent with the trend in stress-relieved samples. Thus, one assumption is that [100] micro-pillars have similar compressive properties with bulk ones. Another possibility is that bulk Mo-Re alloy have large amount of [100] textures after thermal process [7]. Yield stresses in [110] Mo-14Re and Mo-42Re are substantially enhanced due to activated multi-slip bands.

Conclusions

The compressive responses of Mo and Mo-Re alloys are investigated via micro-pillar tests. Solid solution effects of Re on Mo are complex. Solid solution softening happens in low Re content alloys (Mo-5Re). While, solid solution hardening happens in Mo-Re alloys with high Re content (Mo-42Re). Solid solution effects not only depend on Re content, but also depend on the state of samples. What is more, grain orientation / textures still have large influence on the solid solution hardening of Re. Weak strengthening effects are found in [100] Mo-14Re and Mo-42Re. However, the activation of multi-slip planes induces high strength in [110] Mo-14Re and Mo-42Re. In summary, [110] orientation Mo-Re alloys could be considered in condition where high strengthening effect is required.

Data Availability Statement

The data that support the findings of this study are available from the corresponding author, upon reasonable request.

Declaration of Competing InterestsThe authors declare that they have no known competing financial interests or personal relationships that could have appeared to influence the work reported in this paper.

Acknowledgements

This research is funded by Department of Science and Technology of Shaanxi Province, No. QCYRCXM-2022-164, and by National Key R&D Program of China, No. 2022YFB3705403, and by Natural Science Funding of Shaanxi Province, No. 2023-jc-qn-0634.

References

1. X. Chen, R. Li, B. Li, et al. Achieving ultra-high ductility and fracture toughness in molybdenum via Mo₂TiC₂ MXene addition. *Mater. Sci. Eng. A*, 2021, 818, 141422.
2. P. Jehanno, M. Boning, H. Kestler, et al. Molybdenum alloys for high temperature applications in air, *Powder Metal.*, 2008, 51, 99-102.
3. G. Liu, G.J. Zhang, F. Jiang, et al. Nanostructured high-strength molybdenum alloys with unprecedented tensile ductility. *Nature Mater.*, 2013, 12, 344-350.
4. W.B. Guo, G.P. Li, D. Bair, et al. Parametric optimization of multi-pass electron beam melting for molybdenum alloy containing 47.5 wt% rhenium, *Int. J. Refract. Met. H.*, 2023, 113, 106193.
5. H. Yu, H.D. Zhang, L.J. Zhang, Regulation of performance of laser-welded socket joint of Mo-14Re ultra-high-temperature heat pipe by introducing Ti into both weld and heat affected zone, *J. Mater. Res. Technol.*, 2023, 22, 569-584.
6. G. Leichtfried, J.H. Schneibel, M. Heilmaier, et al. Ductility and impact resistance of powder-metallurgical molybdenum-rhenium alloys, *Metall. Mater. Trans. A*, 2006, 10, 2955-2961.
7. X. Yu, P. Hu, K.S. Wang, et al. Microstructure and texture evolution of pure molybdenum during hot deformation, *Mater. Charact.*, 2020, 159, 110010.
8. A. Chaudhuri, A. Sarkar, S. Suwas, et al. Investigation of stress-strain response, microstructure and texture of hot deformed pure molybdenum, *Int. J. Refract. Met. H.*, 2018, 73, 168-182.
9. Y. Xia, P. Hu, K.S. Wang, et al. Dynamic recrystallization behavior of a Mo-2.0%ZrO₂ alloy during hot deformation, *Int. J. Refract. Met. H.*, 2022, 109, 105983.
10. H.R. Xing, P. Hu, Y.H. Zhou, et al. The microstructure and texture evolution of pure molybdenum sheets under various rolling reductions, *Mater. Charact.*, 2020, 165, 110357.
11. M.L. Lobanov, S.V. Danilov, V.I. Pastukhov, et al. The crystallographic relationship of molybdenum textures after hot rolling and recrystallization, *Mater. Design*, 2016, 109, 251-255.

12. A.S. Schneider, B.G. Clark, C.P. Frick, et al. Effect of orientation and loading rate on compression behavior of small-scale Mo pillars, *Mater. Sci. Engineer. A*, 2009, 508, 241-246.
13. Schneider, AS, Frick, CP, Arzt, E, et al. Influence of test temperature on the size effect in molybdenum small-scale compression pillars, *Philos. Mag. Lett.*, 2013, 93, 331-338.
14. J.Y. Kim, D.C. Jang, J.R. Greer, et al. Crystallographic orientation and size dependence of tension compression asymmetry in molybdenum nano-pillars, *Inter. J. Plast.*, 2012, 28, 46-52.
15. J.Y. Kim, J.R. Greer, Tensile and compressive behavior of gold and molybdenum single crystals at the nano-scale, *Acta Mater.*, 2009, 57, 5245-5253.
16. S. Xu, D.Y. Xie, DY, G.S. Liu, et al. Quantifying the resistance to dislocation glide in single phase FeCrAl alloy, *Inter. J. Plast.*, 2020, 132, 102770.
17. J.Y. Kim, D.C. Jang, J.R. Greer, et al. Tensile and compressive behavior of tungsten, molybdenum, tantalum and niobium at the nanoscale, *Acta Mater.*, 2010, 58, 2355-2363.
18. X. Yu, Z. Li, P. Jain, et al. Effect of Si content on the uniaxial tensile behavior of Mo-Si solid solution alloys, *Acta Mater.*, 2021, 207, 116654.
19. Weinberger, CR, Boyce, BL, Battaile, CC, Slip planes in bcc transition metals, *Inter. Mater. Rev.*, 2013, 58, 296-314.
20. N. I. MEDVEDEVA, YU. N. GORNOSTYREV, A. J. FREEMAN. Solid solution softening in bcc Mo alloys: Effect of transition-metal additions on dislocation structure and mobility. *Phys. Rev. B.*, 2005, 72(13): 134107.1-134107.9.
21. J.H. Schneibel, E.J. Felderman, E.K. Ohriner, et al. Mechanical properties of ternary molybdenum-rhenium alloys at room temperature and 1700 K, *Scripta Mater.*, 2008, 59, 131-134.